Nonlinear generation of surface waves against the wind in a limited fetch growth model

A Pushkarev[1,2,3]

[1] LPI, 53 Leninskij Prospekt, 119991, Moscow, Russia
[2] Novosibirsk State University, Novosibirsk, Russia
[3] Waves and Solitons LLC, Phoenix USA

E-mail: dr.push@gmail.com

Abstract. We describe the model for excitation of ocean surface gravity waves by the wind blowing away from the shore. Numerical simulation shows that wave turbulence behaviour can be split in time into two different physical regimes: classical and non-classical one. The classical regime corresponds to self-similar solution developing for the characteristic times defined by ratio of the channel width to characteristic advection velocity of the wave field. The non-classical regime is happening later in time when the energy starts to reflect from the opposite boundary condition and corresponds to energy advection against the wind. It exhibits itself in waves generating predominantly parallel to the shore line, tending to slant toward the shore, as approaching to the beginning of the fetch, at 15 degrees.

1. Model description

We study kinetic equation for waves (Hasselmann equation [1]) for energy spectral density $\varepsilon(\vec{r},\vec{k},t)$, describing nonlinear waves propagation in geometric optics approximation:

$$\frac{\partial \varepsilon}{\partial t}+\frac{\partial \omega_k}{\partial \vec{k}}\frac{\partial \varepsilon}{\partial \vec{r}}=S_{nl}+S_{wind}+S_{diss} \tag{1}$$

for the simplified, but real physical situation, which includes the most important component of the general statement - non-stationarity in time, advection, exact nonlinearity S_{nl}, wind forcing term S_{wind} and wave dissipation term S_{diss} due to wave-breaking.

Such simplified formulation is called the limited fetch wind growth situation, where Hasselmann equation is reduced to

$$\frac{g}{2\omega}\cos\theta\frac{\partial \varepsilon}{\partial x}=S_{nl}+S_{wind}+S_{diss} \tag{2}$$

where $\boldsymbol{x}$ is the spatial coordinate, orthogonal to the shore, and θ is the angle between individual wavenumber $\boldsymbol{k}$ and the axis $\boldsymbol{x}$. This situation is presented schematically on the figure 1:

Content from this work may be used under the terms of the Creative Commons Attribution 3.0 licence. Any further distribution of this work must maintain attribution to the author(s) and the title of the work, journal citation and DOI.
Published under licence by IOP Publishing Ltd

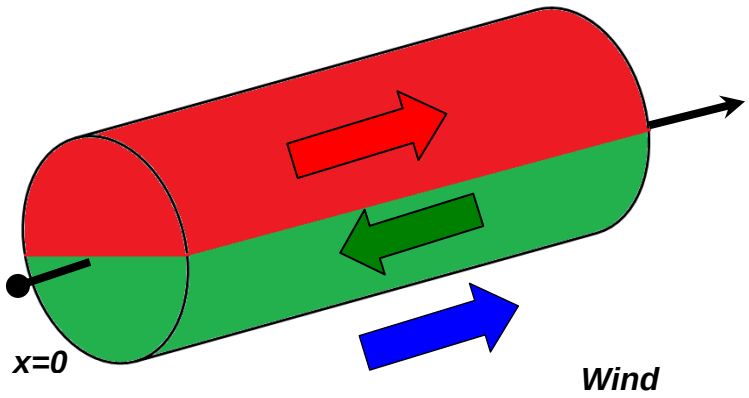

Figure 1. Schematic description of the energy fluxes along the fetch in real and Fourier spaces.

Here black axis presents the real space axis ***x*** orthogonal to the shore line, the red and green cylinder show Fourier space of the system. Red part of the cylinder corresponds to the positive advection velocity in front of time derivative of Hasselmann equation (2) (red arrow is directed away from the shore), while green part of the cylinder corresponds to negative advection velocity (green arrow directed toward the shore), in correspondence with the $\cos\theta$ in equation (2). Such schematic picture suggests that limited fetch growth consists of essentially three different processes happening in real and Fourier spaces: (i) energy advection away the shore in real space (red tube); (ii) energy advection toward the shore in real space (green tube); (iii) nonlinear interaction of the waves between red and green parts of the tube in Fourier space for any given point of the fetch and time.

It is important to use proper boundary conditions for the solution of Caughy problem. We used zero value of the wave field for the red portion of the tube on the left boundary a green portion of the tube on the right boundary. For green portion of the tube on the left and red portion of the tube on the right we used the free energy flux boundary conditions. Physically, such choice of the boundary conditions corresponds to simulation of the waves excitation in the strait of final width by uniform wind blowing orthogonally to the shore.

For the solution of equation (2) we need to know the source terms in its right-hand side. The procedure of exact calculation of S_{nl} term is well-known and given by Webb-Resio-Tracy algorithm [2]. The parameterization of the wind input term S_{in} is given by (see [3]) :

$$S_{wind} = 0.159\frac{\rho_{air}}{\rho_{water}}\omega\left(\frac{\omega}{\omega_0}\right)^{4/3} f(\theta), \quad f(\theta) = \begin{cases}\cos\theta \text{ for-}\pi/2 \le \theta \le \pi/2\\ 0 \text{ otherwise}\end{cases} \tag{3}$$

$$\omega_0 = \frac{g}{u_{10}}, \qquad \frac{\rho_{air}}{\rho_{water}} = 1.3\cdot 10^{-3}$$

and is based on the fact that equation (2) has self-similar solution [3]

$$\varepsilon = x^{p+q}F(\omega x^q) \tag{4}$$

with parameters

$$q = \frac{3}{10}, \quad p = 1 \tag{5}$$

along with the fact of fitting the experimental data by specific regression line, see [4], [5]. The contribution of the dissipation term S_{diss} was calculated similar to [5], where white-capping

dissipation term was introduced implicitly through f^{-5} ($f = \frac{\omega}{2\pi}$) energy spectral tail stretching in frequency range from $f_d = 1.1$ to $f_{\max} = 2.0$.

2. Numerical experiments

We solved Cauchy problem for the Eq.(2) with the following set parameters

- Fetch size 40 km
- Number of nodes 40
- 72 logarithmic frequencies
- 36 points angle resolution
- Wind speed $U_{10} = 5m/\sec$

which translates into:

- Characteristic angular frequency $\omega_{cr} = g/U_{10} = 2rad/\sec$
- Characteristic linear frequency $f_0 = 1.1Hz$
- Dimensionless fetch $\chi = \frac{L}{U_{10}^2} g = 1.6 \cdot 10^4$

Initial conditions were chosen in the form of low-amplitude noise in the red part of the Fourier space and zero in the green part of the phase space cylinder (see figure 1).

Figure 2 represents total energy of the fetch as a function of time. One can see that energy growth evolution can be split into two parts -- first of relatively fast growth for time less than 4 hr, and the second part of relatively slow growth.

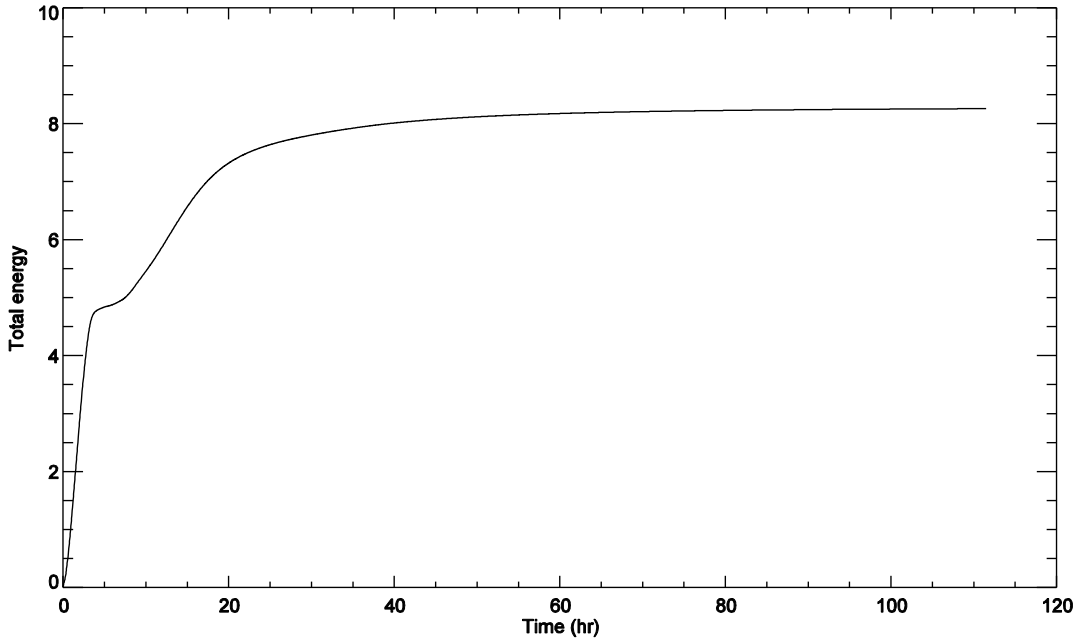

Figure 2. Total energy of the fetch as a function of time.

Comparison of the phase space distributions of the spectrum for *t=2hr* (see figure 5 a,b), and *t=24hr* (see Fig.6 a,b) shows qualitative difference in their shape, too.

For earlier times *t=2hr* the shape of the spectrum has the form of the single hump, growing with the distance from the shore along the fetch. For later time *t=24hr* the shape of the spectrum is more complex: besides classical single-hump energy spectrum, growing away from the shore, one can see side satellites in the form of spikes, corresponding to waves propagating along the shore.

Furthermore, the direction of those waves propagating along the shore is getting slanted toward the shore with the distance diminishing toward the shore. Closer to the shore, the waves are propagating at 15 degrees toward the shore line. This observation is quite remarkable: it means that long enough excitation of the waves in time by the wind blowing away from the shoreline finally excites the waves coming against the wind toward the shore.

Figure 3 represents distribution of energy along the fetch for different times. One can see that energy behavior for time less than *4 hr* is described by threshold-like behaviour propagating along the fetch, in correspondence with [6]**.**

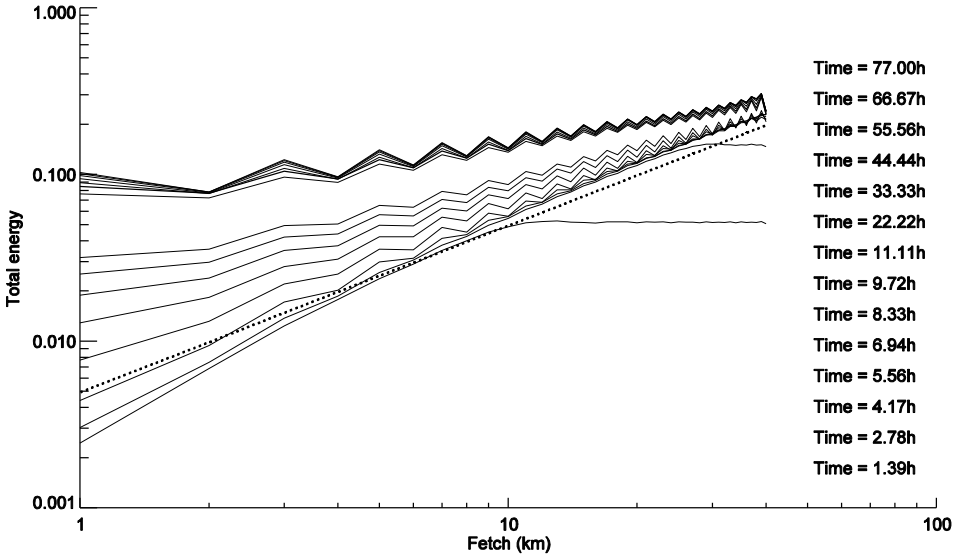

Figure 3. Energy distribution along the fetch. Dotted line -- linear function.

At time around *4 hr*, the energy growth is approximated by linear function of the fetch distance. This dependence was predicted in [7] through self-similarity analysis: it was shown that for fetch-limited self-similar solution the dimensionless energy $\tilde{E} = \dfrac{E \cdot g^2}{U^4} = a\chi$. For time *t = 4 hr*, we get from numerical simulation results $a = 2.4 \cdot 10^{-7}$. Table 1 represents experimental data (see **[7]**) on measuring the constant ***a*** for different experiments. One can see good correspondence of our numerical simulation and experimental predictions in table 1:

Experiment	a
Nakata Bay (Mitsuyasu et al., 1971)	**2.89 × 10−7**
JONSWAP (Hasselmann et al., 1973)	**1.6 × 10−7**
Lake St. Clair (Donelan et al., 1992)	**1.7 × 10−7**
Bothnian Sea (Kahma, 1981)	**2.6 × 10−7**

Table 1. Values of the constant **a** for different experiments

Figure 4 shows mean frequency distribution along the fetch for different moment of time less than *4 hr.* One can see that the portion of the "threshold-like" function is closely described by self-similar solution (4)-(5) :

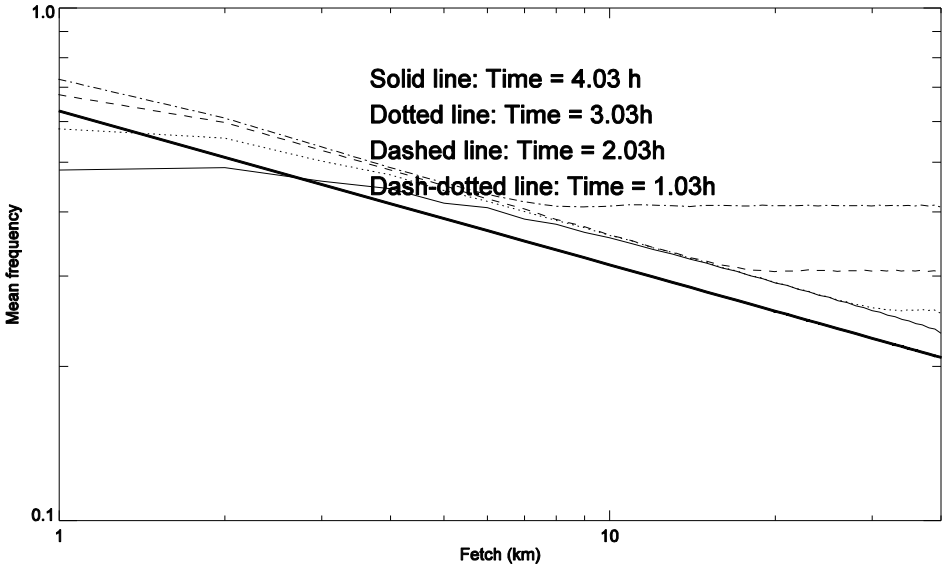

Figure 4. Logarithm of mean frequency distribution as a function of the logarithm of fetch for four different moments of time: 1 hr, 2 hr, 3 hr and 4 hr. Solid line - self-similar prediction q=0.3 from equations (4)-(5)

3. Conclusion

All the above facts clearly show that limited fetch growth in the channels of final width can be split in time into two different physical regimes.

The first regime corresponds to self-similar solution developing for the characteristic times defined by ratio of the channel width to characteristic advection velocity of the wave field and could be called classical. This regime corresponds mainly to energy advection in the red part of the cylinder on figure 1.

The second regime is happening later in time when the energy starts to propagate from the opposite boundary condition and corresponds to energy advection against the wind in the green cylinder on figure 1. It exhibits itself in waves generating predominantly parallel to the shore line, tending to slant toward the shore, as approaching to the beginning of the fetch, at 15 degrees.

One of the most important results of our experiments is the possibility of generation of wind waves against the wind due to nonlinear effects.

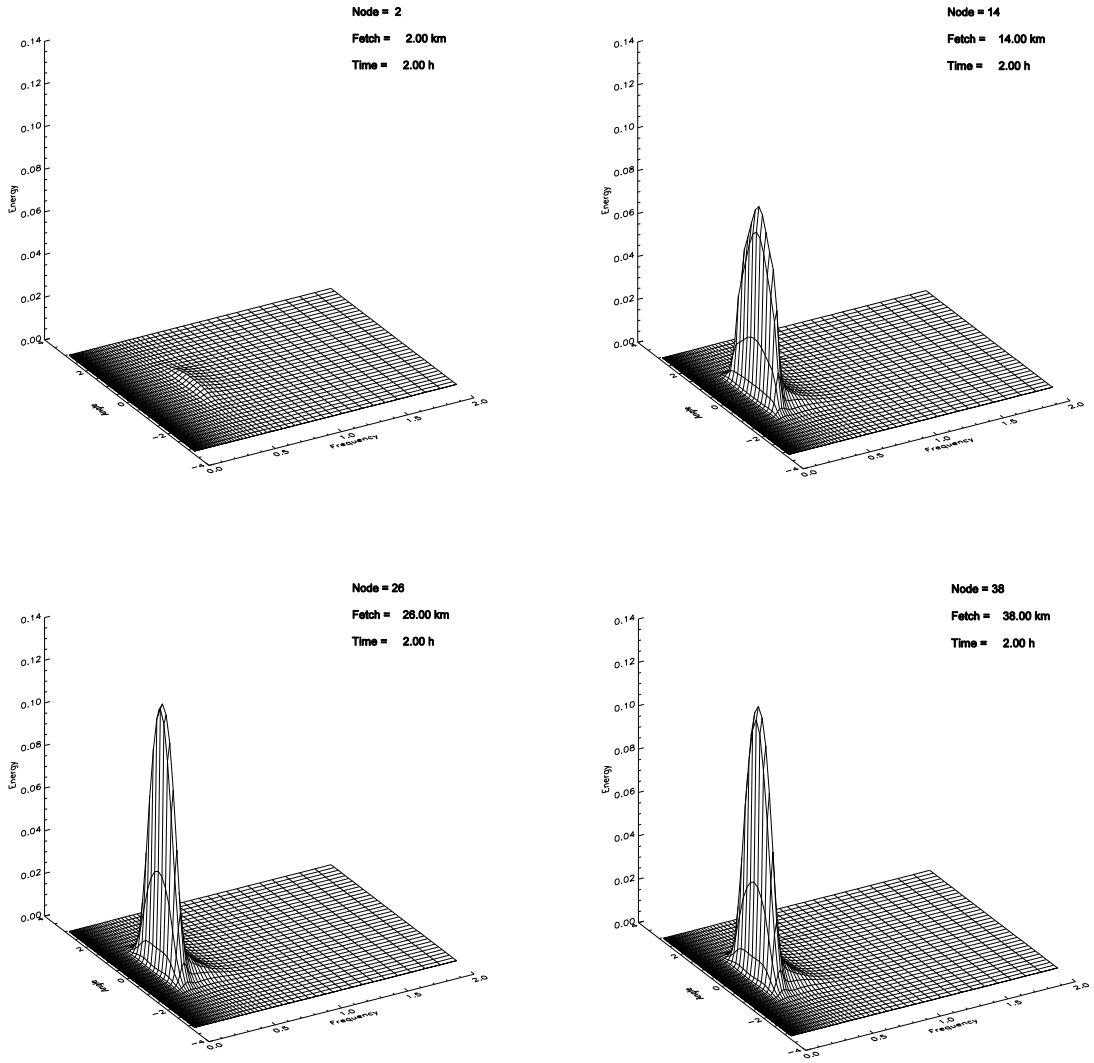

Figure 5a. Spectral energy distribution as a function of frequency f and angle θ at the fetch distances 2 km, 14 km, 26 km, 38 km for time 2hr.

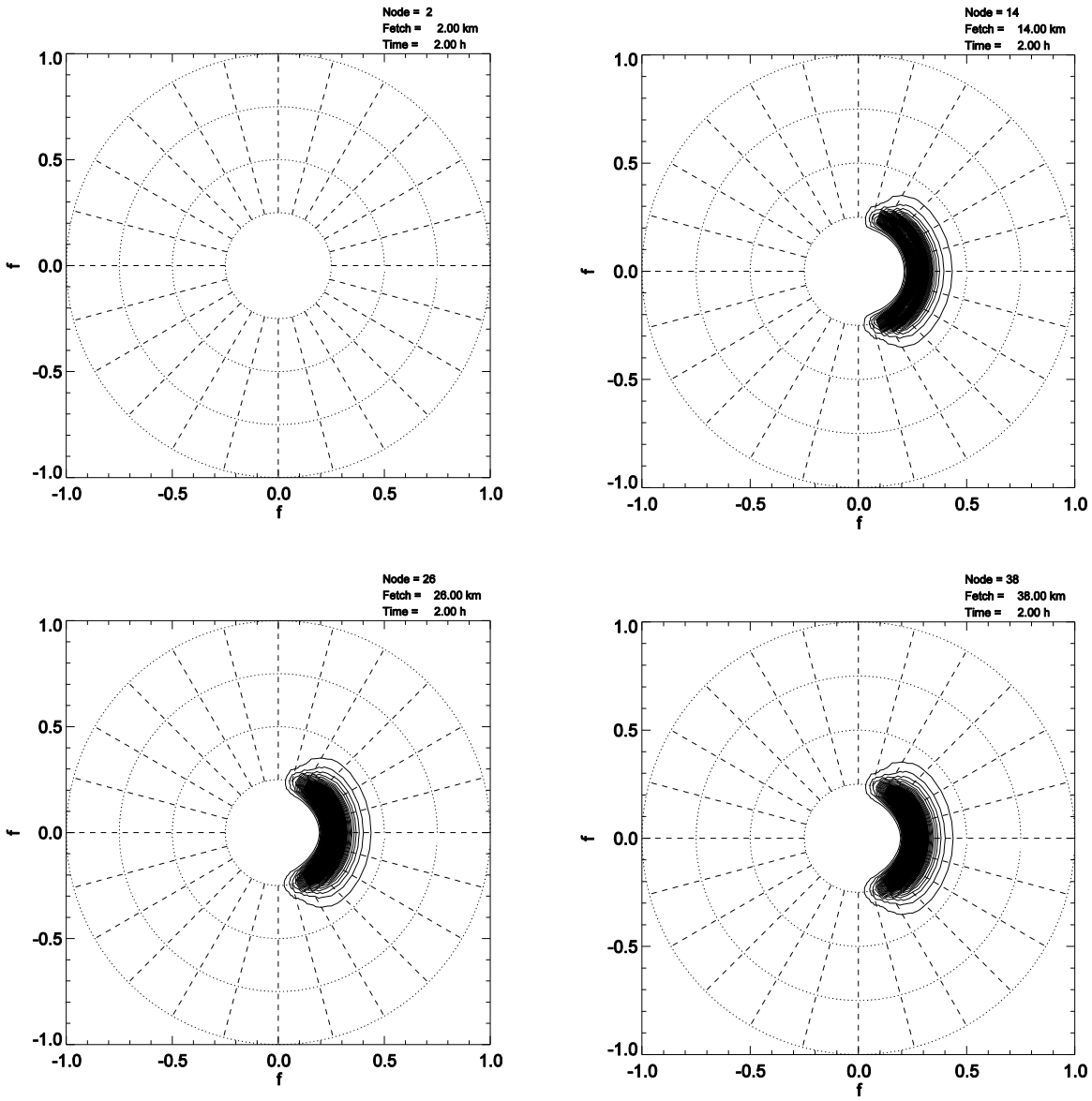

Figure 5b. Spectral energy distribution as a function of frequency f and angle θ in polar coordinates at the fetch distances 2 km, 14 km, 26 km, 38 km for time 2hr.

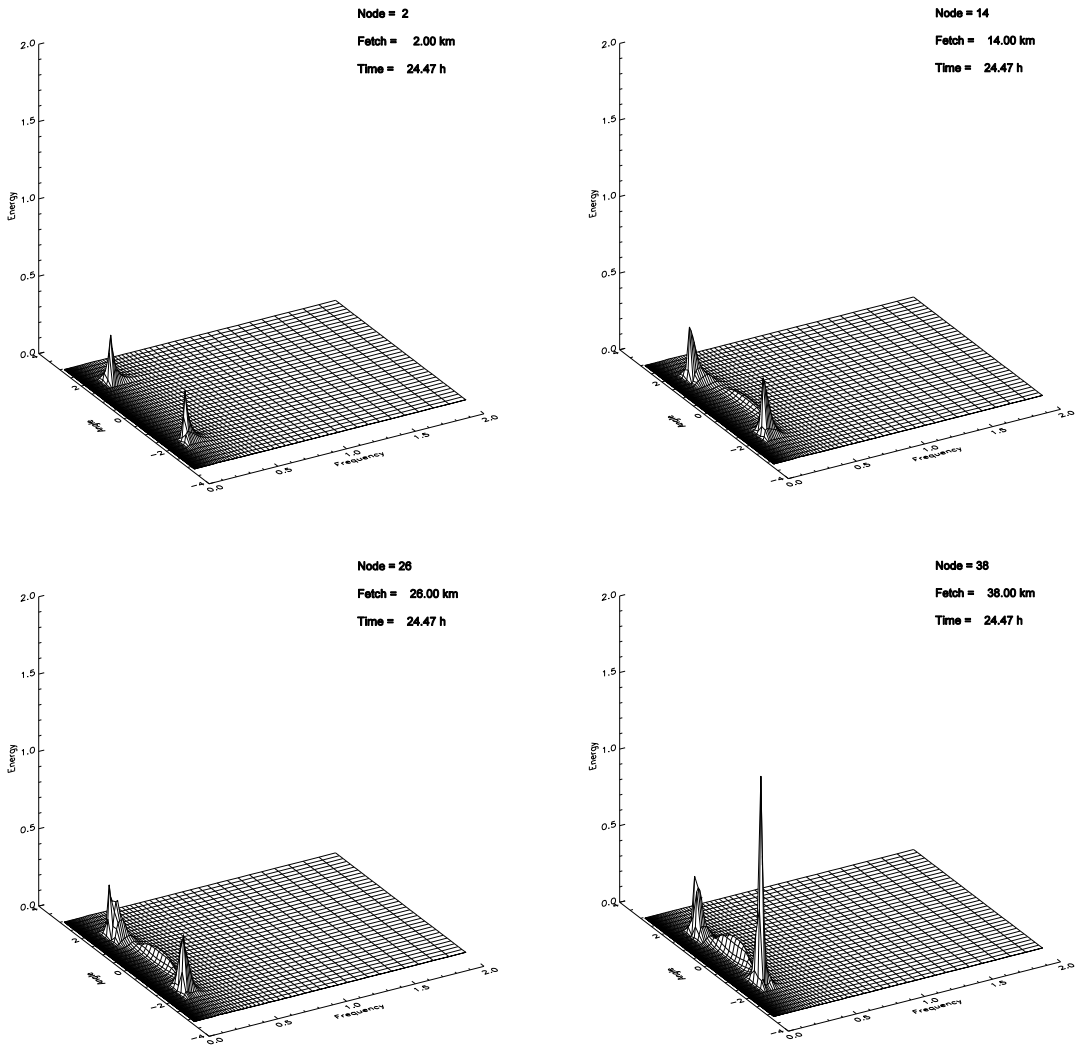

Figure 6a. Spectral energy distribution as a function of frequency f and angle θ at the fetch distances 2 km, 14 km, 26 km, 38 km for time 24.47 hr.

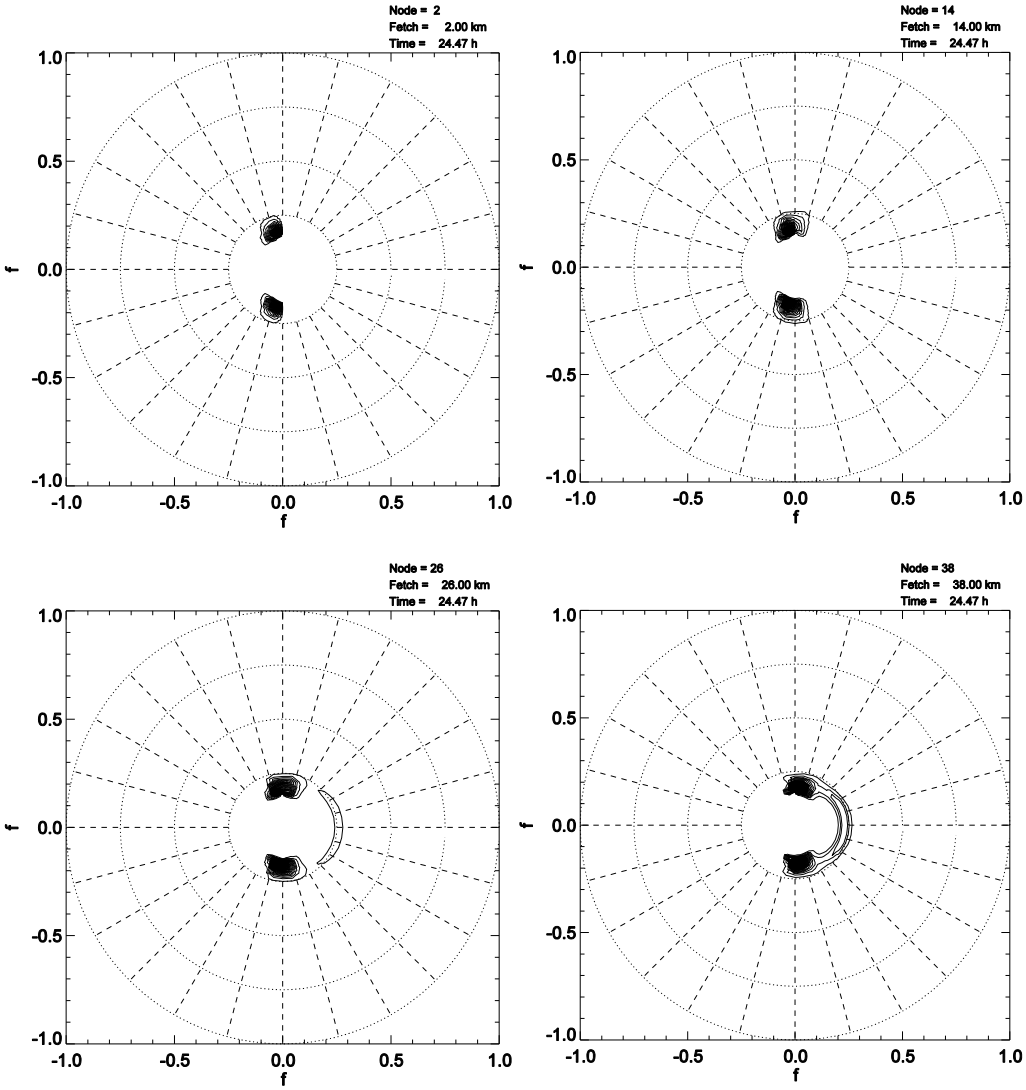

Figure 6b. Spectral energy distribution as a function of frequency f and angle θ in polar coordinates at the fetch distances 2 km, 14 km, 26 km, 38 km for time 24.47 hr.

References

[1] Hasselmann K 1962 On the nonlinear energy transfer in a gravity wave spectrum. Part I *J. Fluid Mech*. **12** 481-500

[2] Tracy B and Resio D 1982 Theory and calculation of the nonlinear energy transfer between sea wavesin deep water *WES Report* **11** U S Army Corps of Engineer

[3] Zakharov V Resio D Pushkarev D 2012 New wind input term consistent with experimental, theoretical and numerical considerations *arXiv:1212.1069 [physics.ao-ph]*

[4] Resio D. and Long C 2004 Equilibrium-range constant in wind-generated spectra *Journal of Geophysical Research* **109** CO1018

[5] Long C and Resio D 2007 Wind wave spectral observations in Currituck Sound, North Carolina *Journal of Geophysical Research* **112** CO5001

[6] Zakharov V and Pushkarev A April 21-25, 2013 Nonlinear generation of surface waves against the wind in a limited fetch growth model *20th meeting WISE*, College Park, Maryland, USA

[7] Zakharov V 2005 Nonlinear Processes in Geophysics **12** 1011–1020

[8] Badulin S, Babanin A, Resio D and Zakharov V 2007 Weakly turbulent laws of wind-wave growth *J. Fluid Mech.* 591 339–378